

Citation for published version:

Alves, IP & Reis, NM 2019, 'Microfluidic smartphone quantitation of *Escherichia coli* in synthetic urine', *Biosensors and Bioelectronics*, vol. 145, 111624. <https://doi.org/10.1016/j.bios.2019.111624>

DOI:

[10.1016/j.bios.2019.111624](https://doi.org/10.1016/j.bios.2019.111624)

Publication date:

2019

Document Version

Peer reviewed version

[Link to publication](#)

Publisher Rights

CC BY-NC-ND

University of Bath

Alternative formats

If you require this document in an alternative format, please contact:
openaccess@bath.ac.uk

General rights

Copyright and moral rights for the publications made accessible in the public portal are retained by the authors and/or other copyright owners and it is a condition of accessing publications that users recognise and abide by the legal requirements associated with these rights.

Take down policy

If you believe that this document breaches copyright please contact us providing details, and we will remove access to the work immediately and investigate your claim.

1 **Microfluidic smartphone quantitation of *Escherichia coli* in synthetic urine**

2 Isabel P. Alves^a, Nuno M. Reis^{b,*}

3 *^aDepartment of Chemical Engineering Loughborough University, Leicestershire LE11 3TU,*
4 *UK*

5 *^bDepartment of Chemical Engineering, University of Bath, Bath BA2 7AY, UK*

6
7 **Corresponding author at: Department of Chemical Engineering, University of Bath,*
8 *Claverton Down, BA2 7AY. Tel: +44 (0) 1225 383 369. E-mail address: n.m.reis@bath.ac.uk*
9 *(N.M. Reis)*

As accepted

Abstract

In spite of the clinical need, there is a major gap in rapid diagnostics for identification and quantitation of *E. coli* and other pathogens, also regarded as the biggest bottleneck in the fight against the spread of antimicrobial resistant bacterial strains. This study reports for the first time an optical, smartphone-based microfluidic fluorescence sandwich immunoassay capable of quantifying *E. coli* in buffer and synthetic urine in less than 25 minutes without sample preparation nor concentration. A limit of detection (LoD) up to 240 CFU/mL, comensurate with cut-off for UTIs (10^3 - 10^5 CFUs/mL) was achieved. Replicas of full response curves performed with 10^0 - 10^7 CFUs/mL of *E. coli* K12 in synthetic urine yielded recovery values in the range 80-120%, assay reproducibility below 30% and precision below 20%, therefore similar to high-performance automated immunoassays. The unrivalled LoD was mainly linked to the 'open fluidics' nature of the 10-bore microfluidic strips used that enabled passing a large volume of sample through the microcapillaries coated with capture antibody. The new smartphone based test has the potential of being as a rapid, point-of-care test for rule-in of *E. coli* infections that are responsible for around 80% of UTIs, helping to stop the over-prescription of antibiotics and the monitoring of patients with other symptomatic communicable diseases caused by *E. coli* at global scale.

Keywords: E. coli detection, Smartphone readout, Point-of-care diagnostics, Synthetic urine, UTIs

1. Introduction

Urinary tract infections (UTIs) are among the most common bacterial infections and pose a significant healthcare burden with *Escherichia coli* (*E. coli*) being the most predominant pathogen in over 80% UTIs (Moreno et al., 2006; Olanrewaju et al., 2017). The differentiation of asymptomatic UTI is subjective and symptoms nonspecific, overlapping with numerous others leading to an overprescription of antibiotics by clinicians, which contributes to retracted and reoccurring UTI crisis and accelerates the pace of multi-drug resistant ‘superbug’ emergence (Center for disease Dynamics, 2015; Cho et al., 2015; Kokkinis et al., 2016). Currently, *E. coli* present concerning resistant levels to the last generation of antibiotics (O’Neill, 2015), however, the current point-of-care (POC) devices for bacterial detection struggle to quantify low limit of detection (LoD) with high sensitivity and specificity enable to early detection of such infections (Cho et al., 2015; O’Neill, 2015). There is therefore a gap in diagnostic tools to quantify directly *E. coli* in biological samples. Lateral flow assays based on colorimetric strips to detect presence of nitrite and microfluidic paper analytical devices (μ PADs) are currently available for a quick screening of UTIs yet lack specificity and provide non-quantitative information.

Diagnosis of UTIs currently relies on clinical sample culture in a centralized laboratory facility, the total procedure requires a minimum of 2-3 days which limits the use of such phenotypic microbiological tests for rapid POC testing (Mairhofer et al., 2009; Olanrewaju et al., 2017). According to the European urinalysis guidelines, the limits for symptomatic UTI from midstream urine caused by *E. coli* is 10^3 CFU/mL (Aspevall et al., 2001; Schmiemann et al., 2010). This is intrinsically difficult to achieve with a conventional ‘dip stick’ test, mostly due to the very small sample volumes used. Bacterial detection can combine other detection principles such as biochemical staining and microscopy (e.g. Tallury et al., 2010; Zourob et al., 2008), other biochemical tests identifying specific metabolites or enzymes (e.g. Tallury et al., 2010; Zourob et al., 2008), immunoassays including ELISA (e.g. Kokkinis et al., 2016; Phan et al., 2018; Su et al., 2015; Tallury et al., 2010; Zourob et al., 2008)) or molecular diagnostics such as PCR (e.g. Chang et al., 2015; Eltzov and Marks, 2016; Kailasa et al., 2019; Tallury et al., 2010; Zourob et al., 2008). These methods are very well understood and widely accepted for pathogen detection, however present long processing times and require expensive laboratory equipment and highly trained users, which is costly and not affordable by all healthcare systems. In addition most of the methods mentioned require several and lengthy steps of sample and reagents preparation. Therefore, there is an unprecedented need for portable

1 and simple approaches to bacteria identification, ideally embedding affordable readout, simple
2 fluid handling and on-chip reagents storage, suited to modern POC diagnostics
3 commercialisation at a global scale (Mabey et al., 2004; Whitesides, 2006).

4 The prevention and early identification of bacterial infections offers the potential for
5 new cost-effective, sensitive, specific and rapid devices to tackle antimicrobial resistance
6 (AMR). Microfluidic devices can bridge the gap between empirical bacteria detection and high
7 precision laboratory equipment by offering integration of multiple steps in one-step assay with
8 portability, sample and reagent volume reduction, increased automation, lower power
9 consumption and higher throughput (Barbosa et al., 2015; Gervais and Delamarche, 2009;
10 Safavieh et al., 2014). There are many successful examples of application of microfluidic
11 devices to several fields such as chemical synthesis, bioanalytics, protein crystallization and
12 POC diagnostics (Mabey et al., 2004; Whitesides, 2006). In spite of its well known advantages,
13 miniaturisation also presents drawbacks, such as high manufacturing costs and reduced optical
14 signal demanding sophisticated readout systems (O'Neill, 2016, 2015). These can involve
15 absorbance, reflectance, fluorescence, surface plasmon resonance (SPR), bio-
16 chemiluminescence and electrochemiluminescence (Roda et al., 2016). The integration of
17 smartphones with a cheap microfluidic device could however work as a cost-effective portable
18 biosensor with tremendous potential for translating diagnostics from centralised labs to POC
19 testing (Roda et al., 2016).

20 The preferable readout approaches in microfluidic immunoassays are based in
21 fluorescence and chemiluminescence due to their excellent sensitivity (Cox et al., 2012;
22 Mairhofer et al., 2009). As an attempt to address the misdiagnosis of bacterial infections, some
23 microfluidic platforms have been previously integrated with smartphones. For instance,
24 Zeinhom et al. (2018) described a sandwich ELISA able to detect *E. coli* O157:H7 in 2h in
25 yoghurt with a claimed detection limit of 1 CFU/mL and in egg with a claimed detection limit
26 of 10 CFU/mL, however the assay in general presented a high background therefore a poor
27 signal-to-noise (SNR) ratio. Cho et al., (2015) developed a bioassay based in a μ PAD with a
28 claimed detection of $1-10^3$ CFU/mL of *E. coli* K12 and *N. gonorrhoea* diluted in urine, however
29 this required several steps of sample preparation with 1% v/v Tween 80 and again the assays
30 presented poor SNR. Rajendran et al. (2014) reported detection of 10^5 CFU/mL *Salmonella*
31 *spp.* and *E. coli* O157 in PBS using biofunctionalized fluorescent nanoparticles. Zhu et al.
32 (2012) published a cell-phone platform with quantum dot enabled to detect 5-10 CFU/mL of
33 *E. coli* O157:H7 in buffer, with total assay taking >1.5 h. In spite of the remarkable LoD

reported on those studies, they all involved complex sample preparation or required extended assays times, both barriers to POC adoption of bacterial testing.

In this study we present a sensitive and rapid optical sandwich fluorescent immunoassay able to detect and quantify *E. coli* K12 in less than 25 minutes in synthetic urine without the need of sample preparation, with the assistance of a smartphone camera. The new sandwich immunosay presents several advantages, such as: 1) affordable off-the-shelf immunoassay reagents, 2) rapid procedure (<25 min), independent on the doubling-time of bacteria, 3) no need for sample preparation and 4) inexpensive microfluidic strips based on an inexpensive, mass-manufacturable Microcapillary Film (MCF) fabricated from FEP-Teflon®, with excellent optical transparency, facilitating smartphone interrogation.

2. Materials and methods

2.1. Reagents and materials

Unconjugated rabbit polyclonal antibody immunogen: O and K antigenic serotypes (all serotypes) of *E. coli* (#PA1-7213) was used as capture antibody (capAb) and the same antibody conjugated with biotin (#PA1-73031) as detection antibody (detAb), both from Fisher Scientific UK Ltd. LB Agar, Miller (#BP1425-2) and LB Broth, Miller (Granulated) (#BPE9723-2) used for microbiological culture, were purchased from Fisher UK. As blocking buffers we have tested the followings products: StartingBlock™ Buffer (#37538), Protein Free (TBS) & blocking Buffer (#37584) from Thermo Scientific (Northumberland, UK); 3% w/w Bovine Serum Albumin lyophilized powder, free of protein (BSA) (#A3858) from Sigma Aldrich (Dorset, UK) in 0.01M PBS; Elisa Synblock (#BUF034A) and Elisa Ultrablock (#BUF033A) were acquired from BioRad (Hertfordshire, UK); JSR Micro B-3001 and JLSP blocking buffers were donated by JSR Micro (Leuven, Belgium). SIGMAFAST™ OPD (o-Phenylenediamine dihydrochloride) tablets (#P9187), Nunc maxisorp ELISA 96-well MTPs (#10547781), 0.01M at pH 7.4 Phosphate Buffer Solution (PBS) (#P5368) and synthetic urine (#S019) were sourced from Sigma Aldrich (Dorset, UK). High Sensitivity Streptavidin–HRP (#21130) were supplied by Thermo Scientific (Northumberland, UK). Enzyme and substrate for fluorescent immunoassay consisted of Alkaline Phosphatase (AP) enzyme substrate supplied by Cambridge Biociences (AnaSpec, # 71101-M) and AttoPhos(R) AP Fluorescent Substrate System (#S1000) purchased from Promega UK (Southampton, UK). As washing buffers, 0.05% v/v Tween 20 diluted in 0.01M PBS (Sigma-Aldrich, Dorset, UK) and alkaline phosphatase KIT wash buffer (AnaSpec #71101-M) (Cambridge Bioscience, UK) were used.

2.2. *E. coli* sample preparation

A colony of *E. coli* K12 “wild type” (NCIMB 11290) was picked up with a sterilized wire loop from a stock culture, inoculated in LB agar and incubated in a orbital shaking incubator under sterile conditions, at 37 °C overnight. Afterwards the culture media was washed 3 times in PBS buffer using centrifugal separation and resuspended in 0.01M PBS or synthetic urine, respectively. *E. coli* sample aliquots were prepared in 2 mL eppendorf with an OD₆₀₀ of 0.7 and stored at -20 °C. Serial dilutions were made from a volume of 0.1 mL *E. coli* samples in PBS and spreaded onto LB agar plates at 37 °C overnight for estimating the cells present in fresh media. Positive and negative control plates with 0.01M PBS and agar without *E. coli* were performed to assess any contamination at this stage.

2.3. MicroCapillary Film (MCF) strips

We used cheap microfluidic strips manufactured from a 10-bore MCF (Figure 1A) using a novel melt-extrusion process by Lamina Dielectrics Ltd. (Billingham, West Sussex, UK) from fluorinated ethylene propylene co-polymer FEP-Teflon®. The MCF material used in this study presented an internal diameter of around 200 µm, with a small 5-6% variability linked to the design of the die and operational conditions used during the continuous manufacturing process (Edwards et al., 2011). MCF presents a high transparency ideal for sensitive optical detection by colorimetric or fluorescence assay and an hydrophobic internal surface that allows simple surface coating of capAb by passive adsorption. Based on the current cost of pelleted FEP of around £20/kg, the material cost for a 40 mm long strip (weighting around 0.2 grams) is negligible. Due to the large surface-to-volume-ratio compared to conventional microwell ELISA platforms and its ‘open microfluidic’ approach (enabling the use of a large volume of sample), high sensitivity is readily achieved.

2.4. Fluorescent *E. coli* sandwich immunoassay

Each reagent was manually aspirated with a 1 mL syringe connected to a MCF strip with a short (10-20 mm) piece of 3 mm i.d. silicon tube. Then, unconjugated polyclonal capture antibody (all serotypes) in PBS 0.01M at a concentration of 40 µg/mL was aspirated through a 200 cm long MCF strip and incubated for 2h at room temperature in a sealed petri dish, to avoid evaporation, followed by 2 mL of protein free (TBS) blocking buffer for another 2h at room temperature. The MCF strip was then washed with 0.05% Tween-20 in PBS and trimmed into small 40 mm long strips. The initial stages of optimisation of the immunoassay performance used a 8-strip fluid handling system, named multi-syringe aspirator (MSA) firstly reported by

Barbosa et al. (2014), extensively adapted to the detection of several biomarkers in the MCF platform (Barbosa et al., 2015; Castanheira et al., 2000). The procedure is further detailed in Supplementary Information. In brief, fluid flow in the MSA is driven by an array of 1 mL plastic syringes. In this study we noticed an advantage in using larger volumes of reagents and/or sample in respect to bacteria capturing and detection, consequently optimised immunoassays were carried out using manual syringes using procedure summarised in Figure 1B. Optimised volumes and incubation times for both MSA and the manual syringe (MS) procedures are detailed in Table 1. For full response curves, a serial dilution of *E. coli* K12 range from 10^8 to 10^0 CFU/mL in 3% w/w BSA or synthetic urine were loaded into a Nunc maxisorp microplate 400 μ L well and 3% w/w BSA used as negative control. The MCF strip was then moved to a new well loaded with 40 μ g/mL biotinylated polyclonal detection antibody (detAb) and washed with 0.05% w/w Tween 20 in 0.1M PBS (Figure 1B). Finally, each strip was incubated with 4 μ g/mL of alkaline phosphatase diluted in Tris-Buffered saline (TBS) at pH 7 before being washed three times with buffer (AnaSpec). Finally, AttoPhos® AP fluorescent was aspirated for yielding an enzymatic fluorescence signal as illustrated in Figure 1C.

2.5. Signal quantification and image analysis

Fluorescence MCF strips were imaged with a BioSpectrum 810 UVP System (AnalytikJena, Cambridge, UK) equipped with a deep-cooled CCD camera using 2 seconds of exposure time. Full response curve in synthetic urine were performed by imaging strips with a smartphone, as shown in Figure 2A. A Super bright 9 LED powered by 3 AAA torch (sourced from Mapplin, UK) was used for exciting the fluorophor and integrated in a black box manufactured in-house. The background signal for fluorescence emission was minimized using a 50 mm square dichroic additive amber filter sourced from Analytik Jena AG (Jena, Germany), place between the MCF strip and the smartphone camera to remove regions of the light spectrum below 430 nm. For smartphone imaging of fluorescence strips, we used a 60x magnification lens with a iPhone 6S attachment sourced from Amazon (Slough, Berkshire). Our simple setup enabled imaging the strips in dark conditions with low fluorescence background and good SNR (Figure 2B). RGB pictures collected with the smartphone's camera were analysed with ImageJ software (NIH, USA) and we noticed the green channel provided maximum SNR (Figure 2B i).

Fluorescence intensity (FI) was calculated from the greyscale pixel intensity, I_{int} for each individual capillary in a given strip, determined from the grey scale plot, an example is

shown in Figure 2B ii). To minimize the intrinsic variability from the smartphone camera settings, I_{int} was normalized by the mean intensity peak of reference strip $I_{int,ref}$ or by the exposure time of camera (which is recorded in the properties of the image file). Fluorescence immunoassay data was presented as fluorescence intensity ratio (FR) is given by the equation (Barbosa et al., 2015):

$$FR = \frac{I_{int,sample}}{I_{int,ref}} \quad (1)$$

AttoPhos® substrate was converted by alkaline phosphatase resulting in an enhancement in fluorescence signal. This is due to increased quantum efficiency, fluorescence excitation and emission spectra that are shifted well into the visible region, according to the manufacturer. We selected AttoPhos® as it presents an unusual large Stokes' shift of 120 nm, which leads to lower levels of background fluorescence and higher detection sensitivity according to the supplier (Promega). FI values were normalized by dividing it with the exposure time of smartphone camera, according to:

$$FI = \frac{I_{int,sample}}{exposure\ time} \quad (2)$$

All immunoassay response curves were fitted with a theoretical 4 parameter logistic model (4PL) and the LoD determined as the minimum concentration yielding as negative control plus 3 times the standard deviation of the blank. Separately, we have considered the impact of SNR (some literature suggests LoD is set by a SNR of 3) on LoD as the former impacts the signal strength and signal stability. By analogy, the limit of quantification (LoQ) was calculated as the lowest concentrations of analyte (blank) plus 10 times the standard deviation (Barbosa and Reis, 2017; Shrivastava and Gupta, 2011).

2.6. Robustness and reproducibility

Robustness and reproducibility of the immunoassay were determined by replicating the same assay in different days. Results translated in terms of inter- and intra-assay variability. The measure of variability of the signal in a give same sample is termed precision and was expressed by the coefficient of variation (CV), obtained from the ratio of the standard deviation to the mean signal. When evaluated on the same assay run this is termed intra-assay variability, whereas different runs lead to inter-assay variability.

In order to evaluate these parameters, three full independent replicates of smartphone fluorescence *E. coli* immunoassay response curves were performed on different days using

different aliquots spiked with the same initial concentration of bacteria. Percentage recovery was calculated based on the ratio of fluorescence intensity (FI) by Equation (2) in 3% w/w BSA to the FI signal in synthetic urine sample.

3. Results and discussion

3.1. Development of colourimetric sandwich immunoassay

In this study we have followed an immunosay detection approach to the quantitation of bacteria in a liquid sample, using *E. coli* as working model, a pathogen responsible for around 80% of UTIs. Due to the considerable size of bacteria (between 0.5 and 5 μm) (Foudeh et al., 2012), a sandwich immunoassay has the additional advantage over small protein quantitation of enabling the use of a single antibody for both detection and labelling of captured *E. coli* cells, by simply varying the conjugation with biotin or other molecule according with the fluorescent or colorimetric signal (Foudeh et al., 2012; Stratz et al., 2014; Wu et al., 2015). There are at least two major drawbacks identified with immunoassay detection of bacteria that explain the very limited success in development of rapid immunoassay tests for bacteria detection. Firstly, bacteria cells display different morphologies with many surface epitopes (proteins, glycoproteins, lipopolysaccharides, and peptidoglycan) that can lead to nonspecific signal interaction with the sensor surface (Ahmed et al., 2014). Secondly, the washing steps essentials for separating removing unbound detAb and enzyme and reducing the background (which sets the LoD) add shear which potentially displaces the captured bacterial cells from the capAb. We have addressed both issues by developing an immunoassay with polyclonal antibodies, which offers the possibility to capturing several O and K *E. coli* serotypes responsible for UTI's and developing multiplexing assays for other related bacteria causing UTI (e.g. *Klebsiella* and *enterobactereace*). In addition, we minimized the potential bacteria displacement caused by shear by incubating detection antibody after the bacterial sample. The sandwich ELISA configuration offers robustness resulting from the capture antibody-bacteria-detection antibody complex (Deshpande, 1996).

We noticed that the optimised conditions for the colourimetric *E. coli* sandwich immunoassay (summarised in Table S1 and further detailed in Supplementary Information document) were similar to those reported previously for protein biomarkers quantitation in the same microfluidic platform (Barbosa et al., 2015, 2014; Gervais and Delamarche, 2009). In particular, the immunoassay was very sensitive to the concentration of 40 $\mu\text{g/mL}$ capAb (Figure S1) and incubation time of detAb, with little effect of enzyme complex. Also, protein-free TBS achieved the best SNR (Figure S2A) and 3% BSA was noted to be the best diluent

for immunoassay reagents (Figure S2B). The immunoassay works with a polyclonal antibody that has the advantage of being strain-specific for few *E. coli* O- and K- serotypes with higher affinity according to supplier informations. Using the microengineering MCF material with multiple bores, we performed 10-replicas on each strip, however it would be possible to coat each capillary with a different capAb and hence use this system to detect a range of bacterial strains within a single assay. We noted similar concentrations of detAb and capAb (40 µg/mL) was paramount to achieving the best performance and 4 µg/mL the best concentration for HSS in colorimetric immunoassay (Figures S2C and S2D). Figure S3A showed a higher SNR was obtained with assay setting 3, consisting of consecutive incubations of the sample (3 min each) followed by 3 min incubation of detAb, a washing step, enzyme complex incubated for 4 min and finally 3 consecutive washings, before addition of Atthophos.

3.2. Development of fluorescence sandwich immunoassay and effect of sample volume

Initial trials with the optimised colourimetric immunoassay summarised in section 3.1 showed very modest performance, with a LoD in the range of 10^5 - 10^6 CFU/mL (so well above the 10^3 - 10^5 CFU/mL required for diagnosis of UTIs) and few reproducibility issues. Consequently, we have adapted the immunoassay to fluorescence quantitation with alkaline phosphatase; we kept the same concentration for enzyme complex (4 µg/mL) and AttoPhos®. Fluorescence immunoassays are widely recognized to present improved LoD in comparison to colorimetric assays (Barbosa et al., 2015; Zeinhom et al., 2018). We noticed a 1,000 fold improvement on the LoD (by reducing the LoD above stated for colourimetric assay 10^5 - 10^6 CFU/mL to a LoD of 136×10^3 CFU/mL in fluorescence assay as shown in Table 2), however reproducibility remained inadequate, presumably due to the high variability in capturing *E. coli* cells which is very dependent of gravity and concentration as we reported recently in Alves and Reis (2019).

We noticed the open microfluidic approach of the MCF strips are uniquely suited to passing a large volume of sample through the microcapillaries coated with capAb. Also, the surface-area-to-volume ratio in a 200 µm internal diameter capillary is about 16 times larger than on a 96 well microtiter plate filled with 100 µl of solution, favouring in-flow bacteria capturing through the formation of complex capAb-bacteria-detAb complex. We noticed fluorescence signal was remarkably improved by incubating the sample multiple times (Figure 3A) during a fixed period instead of a single, longer incubation step (Figure S3). Figure 3B shows full response curves based on multiple steps of sample incubation, this strategy can be easily adopted for diagnosis of UTI due to large volume of urine usually available. We noticed

an improvement in 1-2 orders of magnitude in the LoD by carrying out the full assay with manual syringes instead of the MSA device, we believe this is mostly linked to the ability of using larger volume ($4 \times 350 \mu\text{L}$) of sample in manual syringes setup compared to MSA (with total reagents and sample volume limited to $\sim 1 \text{ mL}$) as summarised in Table 1. The full response curves shown in Figure 3B were obtained for a total of 19 min of assay plus 2 min for AttoPhos® conversion. The LoDs obtained for manual syringes and MSA were 510 CFU/mL and $1.3 \times 10^4 \text{ CFU/mL}$, respectively. The assay variability also remarkably improved using manual syringes, with precision values in general remaining below 20% (Figure 3C). The SNR ratio also improved (Figure 3D), representing an effective increase on sensitivity as can be seen from the 1.5-fold increase on the slope. This effect is easily demonstrated in Figure S3B (in Supplementary Information) where the SNR from a single incubation of *E. coli* spiked in 3% BSA for 12 min was compared with 4 consecutive incubations of same bacterial sample by 3 min each. A 3-fold increase in SNR was obtained for 10^3 CFU/mL with around 6-fold improvement noted for 10^6 CFU/mL , without any negative impact on non-specific (background) signal.

Prior to the development of the rapid and sensitive *E. coli* immunoassay using a smartphone as a readout system, the validation of assay performance in synthetic urine involved fluorescence scanning of the strips with UVP's gel imaging system. Experiments showed a sensitive performance of fluorescent *E. coli* quantification assay without any detrimental effect on background. Table 2 summarised all fluorescent assays carried out in less than 25 min and respective fitting to 4PL correlation, LoD and LoQ. The fluorescent immunoassay in synthetic urine showed 2.5-fold improvement in the LoD, with a LoD of 191 CFU/mL and a LoQ of 575 CFU/mL with an $R^2 = 0.998$, matching a high sensitivity of clinical threshold for an UTI caused by *E. coli*, when compared to non-optimised conditions. Very often, biological matrix effects can interfere in the equilibrium capAb-bacteria-binding. The need of no sample preparation presents multiple advantages in respect to the design of the device and speed of the testing. This remarkable finding can be explained by the surface-area-to-volume-ratio of FEP microcapillary platform that is 4 times larger than any other surface in a microchannel with same internal dimensions. Therefore antibody-antigen binding is favoured by the increased concentration of free binding sites of capAb on the microcapillaries surface, which results in higher assay sensitivity (Castanheira et al., 2015). Nevertheless synthetic urine presents a neutral acidic neutral pH (6-7) that favours antibody activity, promoting the binding with antigen.

3.3. Proof-of-principle of portable smartphone quantification of *E. coli* in synthetic urine

As a first step, the optical detection of converted fluorescent substrate was studied in the smartphone setup and fluorescence calibration curve represented in Support information of this manuscript (Figure S4). The use of the correct environment, light source, angle and design all interfere with the accuracy and sensitivity of a smartphone's camera to image fluorescent strips. A series of 1:2 dilutions of 1 mM of fully converted AttoPhos were loaded into eight 4 cm MCF strips and placed individually into the smartphone setup seen in Figure 2A. At this stage it was determined that the best position of the super bright LED torch was to hold this at the front of the house made dark polyethylene box, hence allowing the light to penetrate along the length of the channels rather than across them. This resulted in sharper images. The control of environmental light is often difficult, producing variability across multiple pictures, so a reference strip with converted AttoPhos was imaged at the same time of the experimental strip, enabling to reduce variability by normalizing the fluorescent signal. These normalized light conditions improved also the image quality capturing caused by variations in the exposure time of the camera (which is usually done automatically by software embedded in the smartphone). Figure 4 shows the results of smartphone fluorescent *E. coli* immunoassays in synthetic urine. Values of LoD and LoQ were described in Table 2, supporting the superior performance of fluorescent bacteria testing in microcapillaries, with a LoD of 240 CFU/mL and a LoQ of 1327 CFU/mL obtained in less than 25 min. Although in line with current expectations for detection of UTI, we observed a slight reduction of 50 CFU/mL in LoD and 572 CFU/mL of LoQ in comparison to imaging with the fluorescence gel scanner.

Previous studies have reported microfluidic fluorescence assay for UTI diagnosis with particular focus to *E. coli* detection and quantitation in buffer, synthetic urine or urine but the assay times used were typically longer, requiring more sample preparation and unable to meet the levels of LoD obtained our work. For example, Yoo et al. (2014) reported a LoD of 10^3 CFU/mL of *E. coli* in PBS using a microfluidic fluorescence assay with total assay taking 30 min plus 45 min for staining. Yang et al. (2011) reported an LoD of 3.4×10^4 CFU/mL of *E. coli* in synthetic urine with total assay taking 100 min. Safavieh et al. (2012) developed a microfluidic loop-mediated isothermal amplification (LAMP) with electrochemical detection presenting an LoD of 48 CFU/mL of *E. coli* involving sample preparation by filtration of urine and total assay time of 60 min.

Robustness and reproducibility of the smartphone fluorescence immunoassay were validated by replicating the same assay on three different days with values translated as inter-

and intra-assay variability as summarised in Figure 4C. The measure of the variability of the signal in the same sample (precision) is termed precision and expressed by the coefficient of variation (CV), which is obtained by the ratio of the average signal and the standard deviation. In general, the precision of the three independent assays remained below 20%, as shown in Figure 4C(i). SNR values presented in Figure 4C(ii) show a slight decrease (around 0.5-fold) when compared to the values achieved for assay in buffer (Figure 3B). This difference was mainly noticeable at the highest concentrations of *E. coli* when the fluorescent signal is proportionally stronger or saturated and harder to be quantified due to limitations with camera detection. Furthermore, intra-assay precision was also evaluated and displayed in Figure 4C(iv), in general it remained below 30%, being slightly higher at lower *E. coli* concentrations in synthetic urine. According to Wild (2013) this is still within an acceptable limit due to cumulative errors effecting the different steps. Recovery values for each concentration showed very linear and consistent within ranges 80-120% (Figure 4C(iii)), meeting the target for high-performance immunoassays. This ultimately demonstrates the fluorescent *E. coli* immunoassay coupled with a smartphone is efficient for *E. coli* quantification in synthetic urine, without any steps of sample preparation. Future developments will be centralized in a new concept of reagents loading to minimize detrimental shear stress on capture of bacterial cells and boost robustness of this microbiological test and develop a portable light detector by developing simple accessories that create a compact dark box around the photo camera, preventing ambient light from interfering with the test's light signal.

4. Conclusions

This work demonstrated proof-of-principle for a new affordable, optical microfluidic test integrated with a smartphone camera able to perform a fluorescence immunoassay quantitation of *E. coli*. Full response curves performed in both buffer and synthetic urine yielded a LoD of up to 240 CFU/mL in less than 25 minutes, which is compatible with clinical cutt-off for UTIs caused by *E. coli*. The ability to pass a large volume of sample through the 'open' microfluidic strips was revealed as key to yielding >100-fold improvement on LoD. This is believed to be linked to increased number of bacterial cells captured by the immobilised capture antibody before addition of immunoassay reagents. The recovery and inter- and intra-variability data demonstrated the bioassay is simple yet robust and reproducible, and comparable to high-performance protein immunoassays. Future work will report strategies for power-free reagents loading and improvement on smartphone fluorescence interrogation, and further validation with clinical urine samples. This affordable immunoassay-smartphone based

strategy for rapid identification of *E. coli* is relevant for fighting the current pace of antibiotic resistance caused by the current empirical prescription of antibiotics worldwide, particularly in low income countries where patients have limited access to centralised microbiology and pathology labs. Further studies using clinical samples and performing cross reactivity tests will be subject of future publications.

Acknowledgements

The authors are grateful to Patrick Hester from Lamina Dielectrics Ltd for providing the MCF material, Dr Ana Isabel Barbosa and Miss Ana Castanheira for advice on coating the FEP microcapillaries, support and training, and Dr Karen Coopman for encouragement and support during the PhD project. This work was funded by Loughborough University internal funds, Santander Mobility Award (Grant No.: C10973/2055) and EPSRC project ([EP/M027341/1](https://doi.org/10.13039/501100011033/EP/M027341/1)) ‘Tackling Antimicrobial Resistance: An Interdisciplinary Approach’.

References

- Ahmed, A., Rushworth, J. V., Hirst, N.A., Millner, P.A., 2014. Biosensors for whole-cell bacterial detection. *Clin. Microbiol. Rev.* 27, 631–646.
<https://doi.org/10.1128/CMR.00120-13>
- Alves, I. P. and Reis, N. M., 2019. Immunocapture of *Escherichia coli* in a fluoropolymer microcapillary array. *J. Chromatogr. A* 1585, 46-55.
<https://doi.org/10.1016/j.chroma.2018.11.067>
- Aspevall, O., Hallander, H., Gant, V., Kouri, T., 2001. European guidelines for urinalysis: A collaborative document produced by European clinical microbiologists and clinical chemists under ECLM in collaboration with ESCMID. *Clin. Microbiol. Infect.* 7, 173–178. <https://doi.org/10.1046/j.1198-743X.2001.00237.x>
- Barbosa, A.I., Castanheira, A.P., Edwards, A.D., Reis, N.M., 2014. A lab-in-a-briefcase for rapid prostate specific antigen (PSA) screening from whole blood. *Lab Chip* 14, 2918–2928. <https://doi.org/10.1039/c4lc00464g>
- Barbosa, A.I., Gehlot, P., Sidapra, K., Edwards, A.D., Reis, N.M., 2015. Portable smartphone quantitation of prostate specific antigen (PSA) in a fluoropolymer microfluidic device. *Biosens. Bioelectron.* 70, 5–14. <https://doi.org/10.1016/j.bios.2015.03.006>
- Barbosa, A.I., Reis, N.M., 2017. A critical insight into the development pipeline of microfluidic immunoassay devices for the sensitive quantitation of protein biomarkers at

the point of care. *Analyst* 142, 858–882. <https://doi.org/10.1039/c6an02445a>

Castanheira, A.P., Barbosa, A.I., Edwards, A.D., Reis, N.M., 2015. Multiplexed femtomolar quantitation of human cytokines in a fluoropolymer microcapillary film. *Analyst* 140, 5609–5618. <https://doi.org/10.1039/c5an00238a>

Deshpande, S. S., *Enzyme Immunoassays: From Concept to Product Development*, Springer Science & Business Media, 1996

Center for disease Dynamics, E.& P., 2015. the State of the World 's Antibiotics. State World 's Antibiot.

Chang, M.S., Yoo, J.H., Woo, D.H., Chun, M.S., 2015. Efficient detection of *Escherichia coli* O157:H7 using a reusable microfluidic chip embedded with antimicrobial peptide-labeled beads. *Analyst* 140, 7997–8006. <https://doi.org/10.1039/c5an01307k>

Cho, S., Park, T.S., Nahapetian, T.G., Yoon, J.Y., 2015. Smartphone-based, sensitive μ PAD detection of urinary tract infection and gonorrhea. *Biosens. Bioelectron.* 74, 601–611. <https://doi.org/10.1016/j.bios.2015.07.014>

Cox, K.L., Devanrayan, V., Kriauciunas, A., Manetta, J., Mantrose, C., Sittampalam, S., 2012. *Immunoassay Methods. Assay Guid. Man.* 43. <https://doi.org/NBK92434> [bookaccession]

E. Moreno, A. Andreu, T.P., , M. Sabate, J.R.J. and G.P., 2006. Relationship between *Escherichia coli* strains causing urinary tract infection in women and the dominant faecal flora of the same hosts. *Epidemiol. Infect.* 134, 1015–1023. <https://doi.org/10.1017/S0950268806005917>

Edwards, A.D., Reis, N.M., Slater, N.K.H., Mackley, M.R., 2011. A simple device for multiplex ELISA made from melt-extruded plastic microcapillary film. *Lab Chip* 11, 4267–4273. <https://doi.org/10.1039/C0LC00357C>

Eltzov, E., Marks, R.S., 2016. Miniaturized Flow Stacked Immunoassay for Detecting *Escherichia coli* in a Single Step. *Anal. Chem.* 88, 6441–6449. <https://doi.org/10.1021/acs.analchem.6b01034>

Foudeh, A.M., Fatanat Didar, T., Veres, T., Tabrizian, M., 2012. Microfluidic designs and techniques using lab-on-a-chip devices for pathogen detection for point-of-care diagnostics. *Lab Chip* 12, 3249–3266. <https://doi.org/10.1039/c2lc40630f>

1 Gervais, L., Delamarche, E., 2009. Toward one-step point-of-care immunodiagnostics using
2 capillary-driven microfluidics and PDMS substrates. *Lab Chip* 9, 3330–7.
3 <https://doi.org/10.1039/b906523g>

4 Kailasa, S.K., Koduru, J.R., Park, T.J., Wu, H.F., Lin, Y.C., 2019. Progress of electrospray ionization and
5 rapid evaporative ionization mass spectrometric techniques for the broad-range identification
6 of microorganisms. *Analyst* 144, 1073–1103. <https://doi.org/10.1039/c8an02034e>
7 Kokkinis, G., Plochberger, B., Cardoso, S., Keplinger, F., Giouroudi, I., 2016. A microfluidic,
8 dual-purpose sensor for in vitro detection of Enterobacteriaceae and biotinylated
9 antibodies. *Lab Chip* 16, 1261–1271. <https://doi.org/10.1039/c6lc00008h>

10 Mabey, D., Peeling, R.W., Ustianowski, A., Perkins, M.D., 2004. Diagnostics for the
11 developing world. *Nat. Rev. Microbiol.* 2, 231. <https://doi.org/10.1038/nrmicro841>

12 Mairhofer, J., Roppert, K., Ertl, P., 2009. Microfluidic systems for pathogen sensing: A
13 review. *Sensors (Switzerland)* 9, 4804–4823. <https://doi.org/10.3390/s90604804>

14 O'Neill, J., 2016. Review on Antimicrobial Resistance: Final report and recommendations.

15 O'Neill, J., 2015. Review on Antimicrobial Resistance. Tackling a Global Health Crisis:
16 Rapid Diagnostics : Stopping Unnecessary Use of Antibiotics. *Indep. Rev. AMR* 1–36.

17 Olanrewaju, A.O., Ng, A., Decorwin-Martin, P., Robillard, A., Juncker, D., 2017.
18 Microfluidic Capillary Circuit for Rapid and Facile Bacteria Detection. *Anal. Chem.* 89,
19 6846–6853.

20 Phan, L.M.T., Rafique, R., Baek, S.H., Nguyen, T.P., Park, K.Y., Kim, E.B., Kim, J.G., Park, J.P., Kailasa,
21 S.K., Kim, H.J., Chung, C., Shim, T.S., Park, T.J., 2018. Gold-copper nanoshell dot-blot immunoassay
22 for naked-eye sensitive detection of tuberculosis specific CFP-10 antigen. *Biosens. Bioelectron.* 121,
23 111–117. <https://doi.org/10.1016/j.bios.2018.08.068>
24 Rajendran, V.K., Bakthavathsalam, P.,
25 Jaffar Ali, B.M., 2014. Smartphone based bacterial detection using biofunctionalized
26 fluorescent nanoparticles. *Microchim. Acta.* <https://doi.org/10.1007/s00604-014-1242-5>

27 Roda, A., Michelini, E., Zangheri, M., Di Fusco, M., Calabria, D., Simoni, P., 2016.
28 Smartphone-based biosensors: A critical review and perspectives. *TrAC - Trends Anal.*
29 *Chem.* 79, 317–325. <https://doi.org/10.1016/j.trac.2015.10.019>

30 Safavieh, M., Ahmed, M.U., Sokullu, E., Ng, A., Zourob, M., 2014. A simple cassette as
point-of-care diagnostic device for naked-eye colorimetric bacteria detection. *Analyst*

139, 482–487. <https://doi.org/10.1039/c3an01859h>

Safavieh, M., Ahmed, M.U., Tolba, M., Zourob, M., 2012. Microfluidic electrochemical assay for rapid detection and quantification of *Escherichia coli*. *Biosens. Bioelectron.* 31, 523–528. <https://doi.org/10.1016/j.bios.2011.11.032>

Schmiemann, Guido, Eberhardt Kniehl, Klaus Gebhardt, Martha M. Matejczyk, E.H.-P., 2010. Diagnosis of urinary tract infections. *Dtsch Arztebl Int* 34, 361–7. <https://doi.org/10.3238/arztebl.2010.0361>

Shrivastava, A. and Gupta, V. B., Methods for the Determination of Limit of Detection and Limit of Quantitation of the Analytical Methods, *Chron. Young Sci.*, 2011, 2, 21–25, <https://doi.org/10.4103/2229-5186.79345>

Stratz, S., Eyer, K., Kurth, F., Dittrich, P.S., 2014. On-chip enzyme quantification of single *Escherichia coli* bacteria by immunoassay-based analysis. *Anal. Chem.* 86, 12375–12381. <https://doi.org/10.1021/ac503766d>

Su, W., Gao, X., Jiang, L., Qin, J., 2015. Microfluidic platform towards point-of-care diagnostics in infectious diseases. *J. Chromatogr. A* 1377, 13–26. <https://doi.org/10.1016/j.chroma.2014.12.041>

Tallury, P., Malhotra, A., Byrne, L.M., Santra, S., 2010. Nanobioimaging and sensing of infectious diseases. *Adv. Drug Deliv. Rev.* 62, 424–437. <https://doi.org/10.1016/j.addr.2009.11.014>

Whitesides, G.M., 2006. The origins and the future of microfluidics. *Nature* 442, 368–373.

Wild, D., 2013. Chapter 1.1 - How to Use This Book, in: Wild, D.B.T.-T.I.H. (Fourth E. (Ed.)., Elsevier, Oxford, pp. 3–5. <https://doi.org/10.1016/B978-0-08-097037-0.00001-4>

Wiseman, M.E., Frank, C.W., 2012. Antibody adsorption and orientation on hydrophobic surfaces. *Langmuir* 28, 1765–74. <https://doi.org/10.1021/la203095p>

Wu, X., Kong, D., Song, S., Liu, L., Kuang, H., Xu, C., 2015. Development of sandwich ELISA and immunochromatographic strip methods for the detection of *Xanthomonas oryzae* pv. *oryzae*. *Anal. Methods* 7, 6190–6197. <https://doi.org/10.1039/c5ay01166c>

Yang, Y., Kim, S., Chae, J., 2011. Separating and detecting *Escherichia coli* in a microfluidic channel for urinary tract infection applications. *J. Microelectromechanical Syst.* 20,

819–827. <https://doi.org/10.1109/JMEMS.2011.2159095>

Yoo, J.H., Woo, D.H., Chun, M.S., Chang, M.S., 2014. Microfluidic based biosensing for *Escherichia coli* detection by embedding antimicrobial peptide-labeled beads. *Sensors Actuators, B Chem.* 191, 211–218. <https://doi.org/10.1016/j.snb.2013.09.105>

Zeinhom, M.M.A., Wang, Y., Song, Y., Zhu, M.J., Lin, Y., Du, D., 2018. A portable smart-phone device for rapid and sensitive detection of *E. coli* O157:H7 in Yoghurt and Egg. *Biosens. Bioelectron.* 99, 479–485. <https://doi.org/10.1016/j.bios.2017.08.002>

Zhu, H., Sikora, U., Ozcan, A., 2012. Quantum dot enabled detection of *Escherichia coli* using a cell-phone. *Analyst* 137, 2541–2544. <https://doi.org/10.1039/c2an35071h>

Zourob, M., Elwary, S., Turner, A., 2008. *Principles of Bacterial Detection, Principles of Bacterial Detection: Biosensors, Recognition Receptors and Microsystems.* <https://doi.org/10.1093/pcp/pcw027>

1 **List of Tables**

2

3 **Table 1** *E. coli* immunoassay steps, conditions and volume range

Bacterial assay in MCF strip	Time (min)	Concentration	Volume (μl)	
			MSA setup	MS setup
<i>E. coli</i> Incubation	12	[10 ⁹ - 10 ¹] CFU/mL	150 × 4	350 × 4
DetAb incubation	3	40 μg/mL	150	250
Washing	-	-	150μl	300
Enzyme incubation	4	4 μg/mL	150	250
Washing	-	-	150 × 3	300 × 3
Enzymatic substrate Incubation	1-5	0.6 mg/mL	150	150
Total assay time		20-25 min		

4

Table 2 Performance of fluorescence immunoassay determined from full response curves for
a *E. coli* concentration of 10^0 - 10^7 CFUs/mL

Sample	Fluidics	Imaging device (fluorescence)	Data correlation with 4PL model (R^2)	LoD (CFU/mL)	LoQ (CFU/mL)	Assay time
Buffer	MSA	Gel scanner	0.999	136×10^3	572×10^3	< 25 min
Buffer	MS	Gel scanner	0.995	473	1300	
Synthetic urine	MS	Gel scanner	0.998	191	575	
Synthetic urine	MS	Smartphone	0.996	240	1327	

Figure captions

Figure 1 FEP-Teflon® microcapillaries platform represented in **A** and *E. coli* quantitative fluorescent immunoassay steps in **B** with final configuration of *E. coli* detection, after conversion of final fluorescent product in **C**.

Figure 2 Smartphone components used for *E. coli* quantitative fluorescent immunoassay and signal image analysis **A** Smartphone set up and accessories to coupled *E. coli* fluorescence immunoassay (i) Super bright 9 LED torch, (ii) dichroic additive amber filter (iii) MCF support (iv) integrated magnified lens (v) smartphone (iPhone® 6S, 12 megapixels camera); **B** fluorescence signal quantitation (i) RGB and green channel image (with reference strip of 0.125 mM Atthophos), (ii) correspondent grey scale analysis.

Figure 3 Comparison of *E. coli* fluorescence immunoassay performance in buffer (3% BSA) using multi syringe aspirator and free range of volumes with single syringes. **A** Principle of affinity used in MCF coated to enhance sensitivity **B** Full response curves for a *E. coli* concentration of 10^0 - 10^7 CFUs/mL **C** Precision range achieved in all *E. coli* concentration tested **D** Signal-to-noise-ratio (SNR) comparison between assays.

Figure 4 Smartphone fluorescence detection of *E. coli* in synthetic urine. **A** RGB and Green channel images of MCF phone quantitation, **B** Full response curve at 2 minutes of Atthophos conversion testing an *E. coli* concentration of 10^0 - 10^7 CFUs/mL, **C** Inter-variability study showing the precision range (i) and SNR overall (ii). Intra-variability study for a triplicate quantitation of *E. coli* in 3 different days showing the percentage of sample recovery in (iii) and intra-assay precision in (iv).

Figures

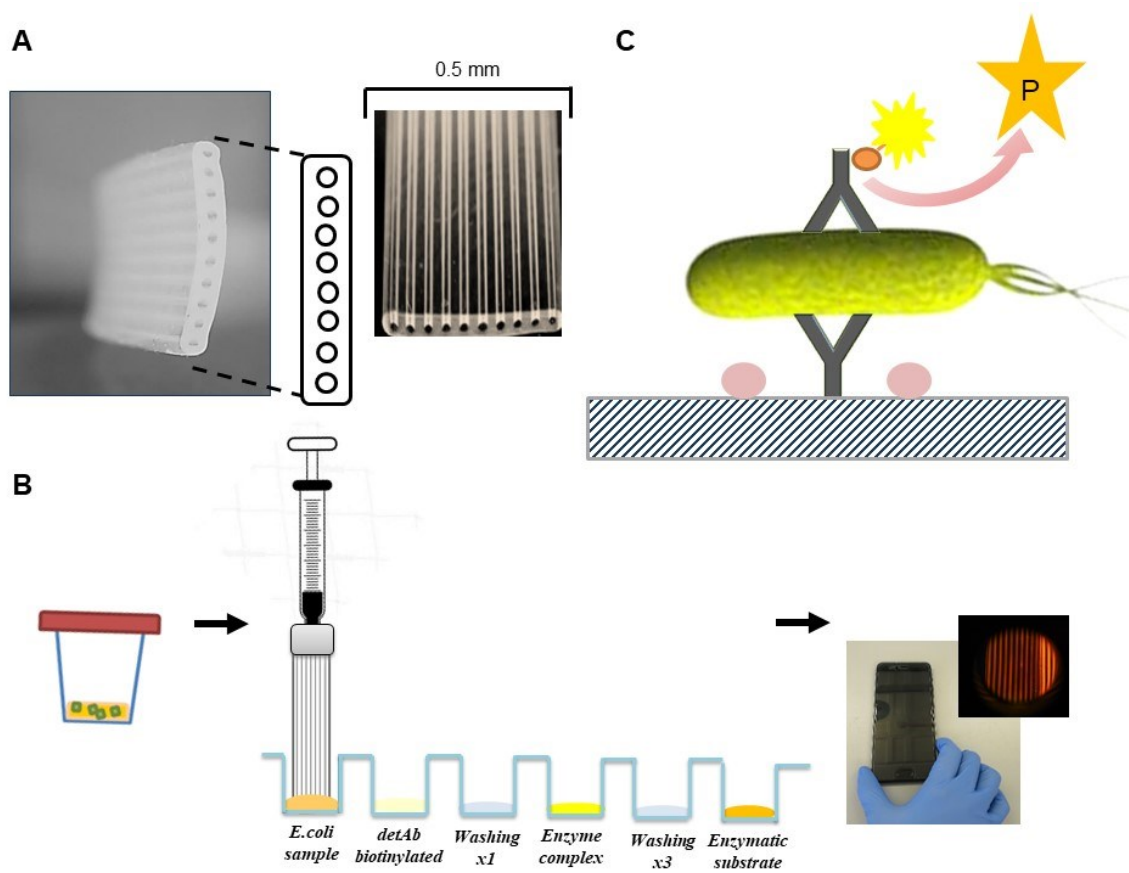
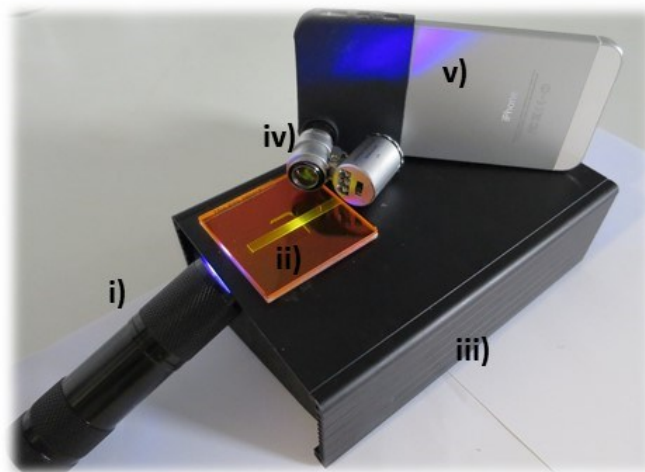


Figure 2

A



B

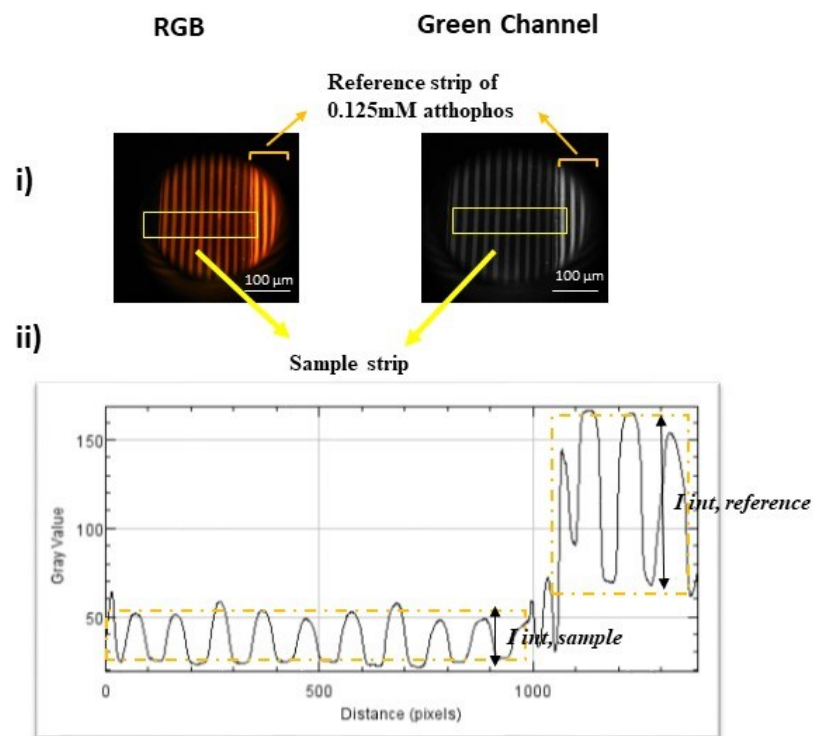


Figure 2

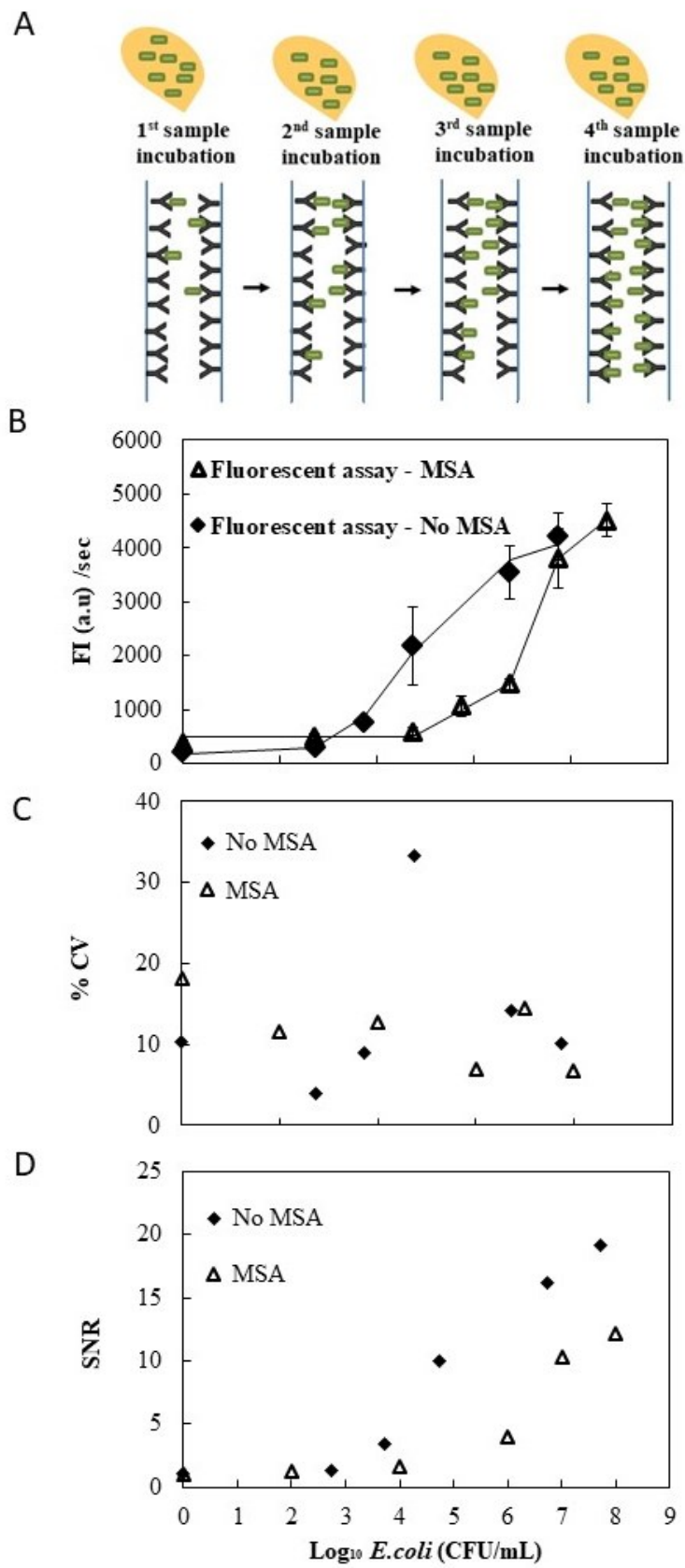


Figure 3

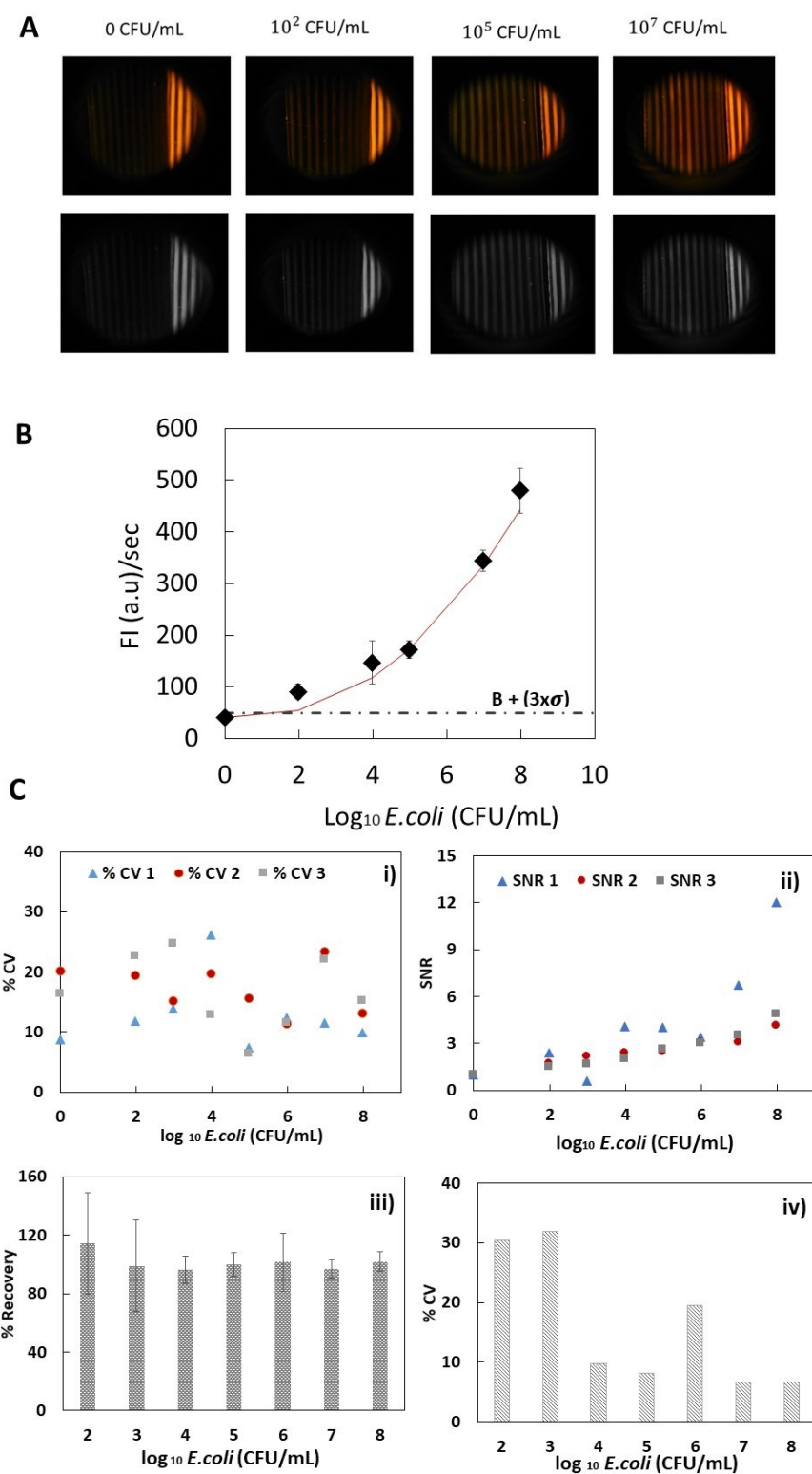


Figure 4